Experimental realization of a low-noise heralded single photon source

G. Brida[1], I.P. Degiovanni[1], M. Genovese[1], A. Migdall[2], F. Piacentini[1], S.V. Polyakov[2], I. Ruo Berchera[1]

[1] *I.N.RI.M., Strada delle Cacce 91, 10135 Torino, Italia and*
[2] *Joint Quantum Institute and National Institute of Standards and Technology,*
100 Bureau Dr, Stop 8441, Gaithersburg, MD, 20899 USA

We present a heralded single-photon source with a much lower level of unwanted background photons in the output channel by using the herald photon to control a shutter in the heralded channel. The shutter is implemented using a simple field programable gate array controlled optical switch.

PACS numbers:

While ideal single-photon sources are desired for many applications from metrology [1], to quantum information [2, 3], to analytical methods, to foundations of quantum mechanics [4] the best that can be achieved are sources that offer some approximation to such a source.

One commonly used approximation is the heralded-photon source which relies on photons produced in pairs, where one of the photons is used to herald the existence of the other photon. While a useful device, this type of source suffers from two particular deficiencies, and these deficiencies have afflicted pair sources from the earliest pair sources based on atomic cascade [5], to parametric down conversion (PDC) [6, 7, 8, 9] in crystals, to four-wave mixing in fibers [10, 11, 12]. One deficiency is that the production is probabilistic and the other is that the probability of extraction of each of the photons of a pair is independent and less than unity. This second deficiency results in many heralding counts that yield no output photon and conversely many photons are emitted from the output channel without a heralding count. Both of these failure modes can present problems for particular applications and are worthy of efforts to reduce their likelihood. Both deficiencies can be reduced by improving the photon extraction efficiency and there are efforts in that direction [7, 13, 14]. To obtain a further reduction in the emission of unheralded photons beyond improving the extraction efficiency, several strategies have been proposed and implemented. For example, using a photon-number-resolving detector on the heralding arm highlights the presence of multi-photon emission from the heralded arm [15]. Another approach exploits the use of an optical shutter, where the optical output path is blocked unless a photon is known to be incident. This simple idea has been discussed for some time [16], but source development efforts have been focused more on the production of single-photon sources "on-demand" [17], rather than on the suppression of unheralded photons. This shuttered or *low-noise* heralded single photon source is particularly advantageous when dealing with detectors with high temporal jitter or slow temporal response (e.g., transition edge superconducting microbolometers), where the low time resolution does not allow for tight time discrimination between the desired heralded photons and unwanted background photons. To compensate for this, data rates must often be reduced to very low levels.

We note that, reducing the noise of a heralded photon source would be of particular advantage in applications such as radiometry where knowing the number of emitted photons is key to the measurements. Noisy photon sources are also problematic for quantum information applications where additional unwanted photons make the already difficult task of processing a fragile quantum state that much more difficult.

In this work we present a heralded-photon source based on PDC with an optical shutter that opens for a short period of time around the expected emission time of a heralded photon. Because this scheme greatly reduces the emission of unheralded photons, we refer to this type of source as a low-noise heralded-single-photon-source (HSPS). Despite the fact that significant further improvements in single-photon performance could be obtained, the current version of our source is already at the level of the best solid-state based single-photon source [18].

In our experimental setup (Fig.1) a continuous wave (cw) laser ($\lambda = 532$ nm) pumps a $5 \times 1 \times 5$ mm periodically poled Lithium Niobate (PPLN) crystal, producing non-degenerate parametric down conversion signal and idler photons with wavelengths of $\lambda_s = 1550$ nm and $\lambda_i = 810$ nm.

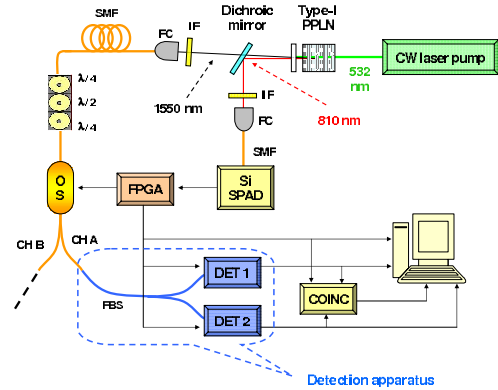The idler photon is sent to an interference filter (IF)

FIG. 1: Experiment arrangement. Channel A is the low-noise HSPS output. Channel B is sent to a beam dump.

with a full width half maximum (FWHM) of 10 nm, then

fiber-coupled to a silicon single-photon avalanche detector (Si-SPAD). The signal photon is addressed to a 30 nm FWHM filter (IF) and coupled to a 20 m long single-mode optical fiber connected to the optical switch (OS) controlled by a field programmable gate array (FPGA). The OS channel A, chosen as our low-noise HSPS output channel, is connected to a 50%-50% fiber beam splitter (FBS) whose outputs are sent to two infrared In-GaAs SPADs (DET_1 and DET_2), triggered by the same FPGA signal that triggers the optical switch. The In-GaAs SPAD detection window is 100 ns long. The outputs of the two InGaAs SPADs are sent to the coincidence electronics and finally recorded by the computer.

The FPGA opens OS channel A for a time interval $\Delta t_{\mathrm{switch}}$ of only a few nanoseconds in coincidence with the detection of an 810 nm photon, and then switches to channel B for a chosen "shuttered" time t_{dead} before the system is ready to be retriggered by a Si-SPAD count.

To reject InGaAs SPAD afterpulses, we set $t_{\mathrm{dead}} = 20$ μs. We note that the minimum time step achievable by our FPGA is $t_{\mathrm{dead}} = 6$ ns, thus, we are far from the performance limits of this technology.

We made measurements with four different switch pulse durations $\Delta t_{\mathrm{switch}}$ (60 ns, 30 ns, 15 ns, and 5 ns).
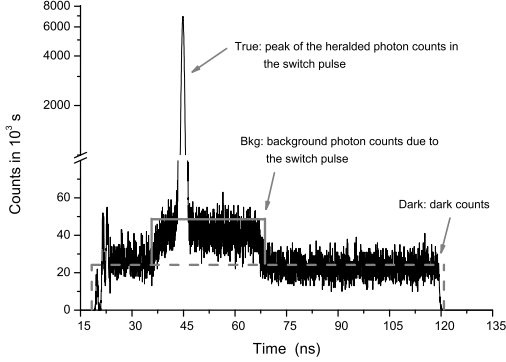

FIG. 2: Histogram of DET_1 detection window, with the peak inside the switch pulse region ($\Delta t_{\mathrm{switch}} = 30$ ns); the true, background, and dark count contributions can be clearly seen.

Looking at the multichannel picture of the detection window of DET_1 (Fig.2) we can distinguish three different "regions" corresponding to:

- $N^{(\mathrm{True})}$ = true heralded photon counts;

- $N^{(\mathrm{Bkg})}$ = counts due to background and stray light passing through the optical switch;

- $N^{(\mathrm{Dark})}$ = dark counts of the IR detector.

We define the true heralded photon detection probability for each trigger count as

$$P_i^{(\mathrm{True})} = \frac{N^{(\mathrm{True})}}{N_i^{(\mathrm{Trig})}} \qquad i = 1, 2 \qquad (1)$$

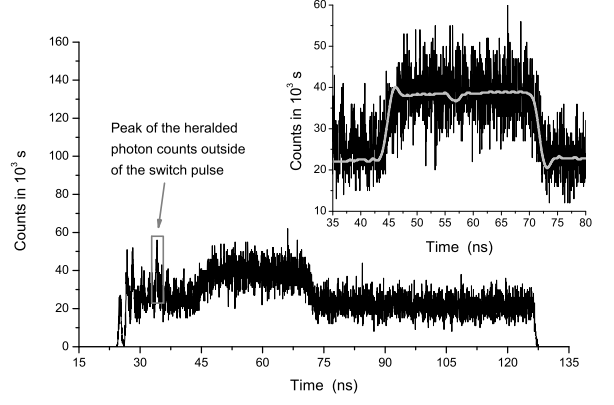FIG. 3: Histogram of DET_1 detection window ($\Delta t_{\mathrm{switch}} = 30$ ns) when the heralded photons peak is outside of the OS active region, therefore being highly suppressed. The inset shows the switch-on region, with the solid line showing the shape of the electrical pulse driving the OS.

($P_i^{(\mathrm{Bkg})}$ and $P_i^{(\mathrm{Dark})}$ are analogously defined), where $N_i^{(\mathrm{Trig})}$ is the total number of trigger counts accepted by the i-th detector.

The overall detection probability of detector i is

$$P_i^{(\mathrm{Tot})} = P_i^{(\mathrm{True})} + P_i^{(\mathrm{Bkg})} + P_i^{(\mathrm{Dark})}. \qquad (2)$$

To evaluate these three probabilities, we look at the histogramed outputs of DET_1 and DET_2 in two different configurations: *peak-in* (Fig.2), with the heralded photons arriving in correspondence of the OS active region, and *peak-out* (Fig.3), where the switching pulse is delayed with respect to the arrival of the heralded photons so that they do not arrive during the switch open time (i.e. the pulse duration $\Delta t_{\mathrm{switch}}$).

We can then calculate the ratio of unwanted to total photons in our distribution channel: we call this parameter *Output Noise Factor* (ONF), defined as:

$$ONF = \frac{P_1^{(\mathrm{Bkg})} + P_2^{(\mathrm{Bkg})}}{P_1^{(\mathrm{True})} + P_1^{(\mathrm{Bkg})} + P_2^{(\mathrm{True})} + P_2^{(\mathrm{Bkg})}}. \qquad (3)$$

The other figure of merit that we consider for our HSPS is α (analogous to the second order correlation function $g^{(2)}(0)$ [19]):

$$\alpha = \frac{P_{12}^{(\mathrm{True+Bkg;True+Bkg})}}{P_1^{(\mathrm{True+Bkg})} \cdot P_2^{(\mathrm{True+Bkg})}}, \qquad (4)$$

where $P_{12}^{(\mathrm{True+Bkg;True+Bkg})}$ is the probability of a coincidence photon count between DET_1 and DET_2 (dark counts subtracted). Assuming $P_{12}^{(\mathrm{True;True})} = 0$ (there is only one heralded photon in the fiber beam splitter per heralding count), and $P_i^{(\mathrm{Bkg})}$ and $P_i^{(\mathrm{Dark})}$ are independent, we obtain:

$$P_{12}^{(\mathrm{True+Bkg;True+Bkg})} = P_{12}^{(\mathrm{Tot;Tot})} - P_{12}^{(\mathrm{Dark;tot})} -$$

$$-P_{12}^{(\text{Tot;Dark})} + P_{12}^{(\text{Dark;Dark})}. \tag{5}$$

All the terms in Eq.() can be extracted from measurements made by blocking the light to each detector in turn.

Our results, summarized in Figs. 4 and 5, show the ONF decreasing linearly with the duration of Δt_{switch}, a direct consequence of the reduction in background photons as the OS on-time is narrowed. The values range from a maximum of 11.5% for $\Delta t_{\text{switch}} = 60$ ns to a minimum of 1.45% for $\Delta t_{\text{switch}} = 5$ ns, clearly showing the noise reduction in our source's output channel.
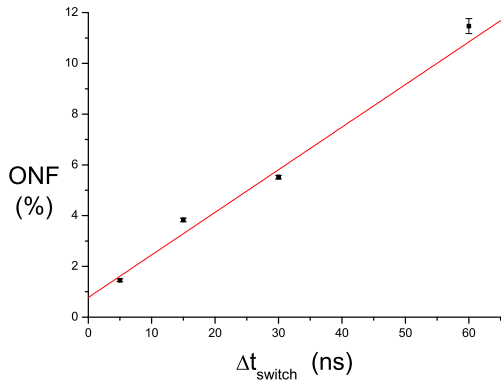

FIG. 4: ONF parameter as a function of the switching time Δt_{switch}. The linear fit (line) of the data (points) shows a correlation factor $R = 0.985$.

As expected, the parameter α shows the same behavior as the ONF, decreasing linearly with the switching time Δt_{switch}: it ranges from 0.253 ($\Delta t_{\text{switch}} = 60$ ns) to the remarkable value 0.0136 ($\Delta t_{\text{switch}} = 5$ ns), highlighting the advantage of our shuttered single-photon source. In fact, our best measured α value ($\alpha = 0.0136$) is comparable with, or even better than, the best values obtained for single-photon emitters such as for example, a quantum dot in micropillar presenting $\alpha = 0.02$ [20] or $^{40}\text{Ca}^+$ in ion-trap cavity presenting $\alpha = 0.015$ [21]. Fig. 5 shows a linear fit to the data, where for the ideal case of $\Delta t_{\text{switch}} = 0$, we would obtain $\alpha = -0.003 \pm 0.025$, which is clearly compatible with 0, indicating that there are no other effects limiting the device performance to this level of uncertainty.

Here, the uncertainties on the α data are larger than those obtained for the ONF, mainly because the double coincidence events needed to evaluate $P_{12}^{(\text{True+Bkg;True+Bkg})}$ are relatively rare. This further highlights the extremely low noise of our HSPS.

The main performance limitation, i.e. the lower bound for α that we achieved, is due to the slow rise/fall time of our pulse generator (≈ 2.5 ns, as seen in the inset plot of Fig. 3) and the jitter of the Si-SPAD in the heralding arm (≈ 500 ps). Each of these limits how many non heralded photons can be rejected. The first by providing a minimum width of the switch open time and the second

by adding uncertainty in the time between the opening of the switch (driven by the heralding events) and the presence of the heralded photon. This jitter is directly related to the spreading of the true coincidences peak (True) and clearly, Δt_{switch} must be kept larger than the full width of the peak itself (currently ≈ 3 ns).

These are technical rather than fundamental issues that can be overcome by using lower jitter commercially available Si-SPADs along with faster pulse generators leading to a possible $\Delta t_{\text{switch}} \lesssim 1$ ns. From the linear trend in Figs. 4 and 5 we would expect, at that peak width, the values of ONF to be within 1 % of zero and α to be within 0.02 of zero at the 1 ns widths that we believe are achievable.
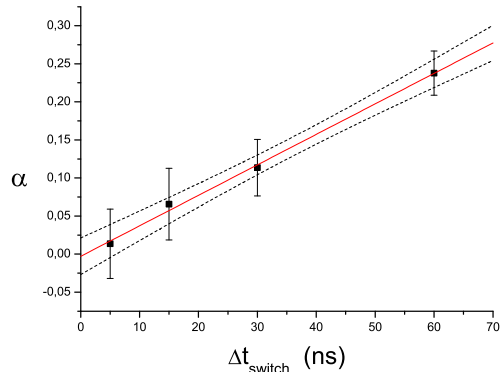

FIG. 5: Behavior of the parameter α ($\approx g^{(2)}(0)$) as a function of the switching time Δt_{switch} (expressed in nanoseconds). The linear fit (solid line) of the data (points) shows a correlation factor $R = 0.998$, along with 95% confidence bands (dashed curves).

To investigate the extinction performance of our OS, we compare the heralded photon peak within the switch on-time as in Fig. 2 with the corresponding residual peak of the heralded photon when it is out of the switch pulse duration as in Fig. 3, defined as the ratio between $P^{(\text{True})}$ in peak-out and peak-in configurations:

$$r = \frac{P_{\text{peak-out}}^{(\text{True})}}{P_{\text{peak-in}}^{(\text{True})}}. \tag{6}$$

Our measured r value of 3.5×10^{-3} means that our source produces background counts at a rate of just 37 Hz, this value is comparable to the lowest dark count rate of the best Si-SPADs currently available.

The calibration of our detection apparatus, composed of the fiber beam splitter and the two InGaAs SPADs, is made using a power-stabilized 1550 nm laser beam attenuated to the photon counting regime, giving an overall detection efficiency $\eta = (8.1 \pm 0.2)\%$ [22]. This calibration allows us to evaluate the coupling efficiency γ of our

single-photon source, defined as:

$$\gamma = \frac{P_1^{(\text{True})} + P_2^{(\text{True})}}{\eta}. \tag{7}$$

The average of the coupling efficiencies obtained for each OS configuration is $\gamma = (14 \pm 1)\%$, and the singles measurements are independent from Δt_{switch}. We emphasize that better engineering could increase γ significantly [14].

In conclusion, we have presented an experimental implementation of a low-noise heralded single-photon source. The results obtained in terms of the single-photon parameters α and ONF are already comparable with the best solid-state based single-photon sources [18]. As implemented, α and ONF are limited by the rise/fall time of the pulse generator controlling the optical switch and the jitter of the heralding detector, resulting in a minimum switch window of a few nanoseconds.

In addition, further improvements in α and ONF are expected with readily available components such as a detector with less than 100 ps jitter and an optical switch with sub-ns switching times. We note that the inherent switching time of the optical switch used was 18 GHz.

We also note that, with respect to the other single-photon sources such as for example quantum dots, color centers in nanodiamond, etc. [18], the low-noise heralded-single-photon source has the advantage of wide wavelength tunability typical of PDC-based sources. Furthermore, because this source operates at telecom wavelengths, it can exploit commercially available telecom components, e.g., wavelength division multiplexing and/or narrow spectral selection by means of Bragg fiber filters.

The background photon rejection and the possibility of controlling and tuning the value of t_{dead} is particularly advantageous when dealing with slow response systems or slow detectors, such as for example, detectors with high temporal jitter or slow temporal response like transition edge superconducting microbolometers [23], where the slow response does not allow for temporal discrimination of unwanted events and thus the system is forced to operate at impractically low data rates.

Finally, the whole system can be integrated, or at least pigtailed, as the source can be realized with a PPLN waveguide, the same technology used for the fast OS.

[1] http://www.quantumcandela.net; G. Brida *et al.*, Laser Phys. Lett. **3**, 115 (2006); S. V. Polyakov and A. L. Migdall, J. Mod. Opt. **56**, 1045 (2009) *and ref.s therein.*

[2] N. Gisin and R.Thew, Nature Photon. **1**, 165, (2007) *and ref.s therein.*

[3] J. L. O'Brien, A. Furusawa, J. Vickovic, Nature Photon. **3**, 687, (2009) *and ref.s therein.*

[4] M. Genovese, Phys. Rep. **413**, 319, (2005) *and ref.s therein.*; G. Brida *et al.*, Opt. Express, **16**, 11750 (2008); G. Brida *et al.*, Phys. Rev. A, **79**, 044102 (2009).

[5] P. Grangier, G. Roger, and A. Aspect, Europhys. Lett. **1**, 173 (1986).

[6] D. N. Klyshko, Kvant. Electron. **7**, 1932 (1980); C. K. Hong and L. Mandel, Phys. Rev. Lett. **56**, 58 (1986); A. B. U'Ren, C. Silberhorn, K. Banaszek, and I. A. Walmsley, ibid. **93**, 093601 (2004).

[7] S. Castelletto, I. P. Degiovanni, V. Schettini, and A. Migdall, Opt. Express **13**, 6709 (2005).

[8] S. Fasel et al., New J. Phys. **6**, 163 (2004).

[9] A. B. U'Ren, C. Silberhorn, J. L. Ball, K. Banaszek, and I. A. Walmsley, Phys. Rev. A 72, 021802(R) (2005).

[10] G. P. Agrawal, *Nonlinear Fiber Optics*, 2nd ed. (Academic Press, New York, 1995).

[11] J. Fan and A. Migdall, Opt. Express **15**, 2915 (2007); J. Fan, M. D. Eisaman, and A. Migdall, Phys. Rev. A **76**, 043836 (2007); Opt. Express **15**, 18339 (2007).

[12] J. Fulconis, O. Alibart, J. L. OBrien, W. J. Wadsworth, and J. G. Rarity, Phys. Rev. Lett. **99**, 120501 (2007).

[13] C. Kurtsiefer, M. Oberparleitner, and H. Weinfurter, Phys. Rev. A 64, 023802 (2001); F. A. Bovino, P. Varisco, M. A. Colla, G. Castagnoli, G. Di Giuseppe, and A. V. Sergienko, Opt. Commun. 227, 343-348 (2003); S. Castelletto, I.P. Degiovanni, A. Migdall and M. Ware, New J. Phys. 6, 87 (2004).

[14] A. Fedrizzi et al., Opt. Express 15, 15377 (2007).

[15] T. Horokiri, Y. Takeno, A. Yabushita, and T. Kobayashi, Phys. Rev. A. **76**, 012306 (2007).

[16] A. Migdall, Phys. Today **52**, 41 (1999).

[17] A. L. Migdall, D. Branning, and S. Castelletto, Phys. Rev. A **66** 053805 (2002); E. Jeffrey, N. A. Peters, and P. G. Kwiat, New J. Phys. **6**, 100, (2004). S. Takeuchi, R. Okamoto, and K. Sasaki, Appl. Opt. **43**, 5708 (2004).

[18] M. Oxborrow and A. C. Sinclair, Contemp. Phys. **46**, 173 (2005); S. Scheel, J. Mod. Opt. **56**, 141 (2009).

[19] P. Grangier, G. Roger, and A. Aspect, Europhys. Lett. **11**, 173 (1986); G. Brida *et al.*, Phys. Lett. A **328**, 313 (2004).

[20] J. Vuckovic, *et al.* Appl. Phys. Lett. **82**, 3596 (2003); A. J. Bennett, *et al.* Opt. Express **13**, 50 (2003).

[21] M. Keller, *et al.* Nature (London) **431**, 1075 (2004).

[22] All the uncertainties and the error bars correspond to the coverage factor $k = 1$ except for the 95% confidence bands of Fig. 5.

[23] R. H. Hadfield, Nature Photon. **3**, 696, (2009) *and references therein.*